Simulation of bioaugmentation involving exogenous bacteria injection

Sookyun Wang
Environmental Research Institute, Ewha Womans University, Seoul, Korea

M. Yavuz Corapcioglu
Department of Civil Engineering, Texas A&M University, College Station, Texas, USA

Received 20 December 1999; revised 21 March 2002; accepted 4 April 2002; published 17 December 2002.

[1] The degradation of organic hydrocarbons through microbial reactions in subsurface environments has been widely studied in the literature. Most studies, however, have focused on biostimulation, which aims to enhance biodegradation by indigenous bacteria. This study presents a mathematical model to simulate the fate and transport of a reactive contaminant degraded through cometabolism during the in situ bioaugmentations involving the injection of nutrients and/or exogenous bacteria. We incorporate hydrogeologic factors affecting the transport of contaminant as well as microbial metabolic reactions into the model. Modified Monod kinetics and a microcolony concept are used to investigate the effects of mobile bacteria in the aqueous phase and bacteria attached on solid surfaces on the transport and biodegradation of an organic contaminant. Permeability reduction due to microbial accumulation in pore spaces and its effect on the biodegradation processes are examined by performing a numerical experiment involving in situ biodegradations by exogenous bacteria. The effect of bacteria as biosorbents is also considered in model formulations to investigate the biocolloid-facilitated transport of a contaminant. The two-dimensional governing equations are solved numerically using a fully implicit finite difference method with an alternating direction implicit scheme. For model evaluation purposes, a model comparison is performed against an independently developed biodegradation model and showed remarkably close matches in the concentration profiles. The model is applied to a case study to demonstrate its behavior. The results of simulations show significant effects of bioaugmentative operations on the fate and distribution of all the chemical species and biomass and their interactions. In addition to the enhanced efficiency caused by the operation, operation-induced limitations such as permeability reduction is also demonstrated. Factors determining the overall biodegradation rate include the bioavailability of the contaminant and the distribution of biomass and relevant chemical species. The overall results implied that the success of in situ bioaugmentation depends on how to control the contact of biodegrading microbes with contaminants and how to supply enough nutrients into the contaminated zone and stimulate microbial activities. *INDEX TERMS:* 1831 Hydrology: Groundwater quality; *KEYWORDS:* bioaugmentation, modeling, biobarrier, bacteria, hydraulic conductivity

Citation: Wang, S., and M. Y. Corapcioglu, Simulation of bioaugmentation involving exogenous bacteria injection, *Water Resour. Res.*, *38*(12), 1293, doi:10.1029/2001WR000344, 2002.

1. Introduction

[2] The contamination of groundwater and soils due to the infiltration of hazardous organic chemicals into the subsurface has been an issue of great interest and importance for public health. Although various remediation techniques have been proposed and employed to treat subsurface contaminants, some are economically impractical or need to be applied to field-scale experiments to prove their effectiveness. In the last few decades, in situ biodegradation has received significant attention as a contaminant removal technique that is relatively low in cost, as well as an efficient and safe tool for removing organic contaminants in the subsurface. Recognition of the capabilities of microorganisms, particularly bacteria, has been well studied by researchers subsequent to *ZoBell*'s [1946] review of the hydrocarbon utilization of microorganisms. Widespread in nature, bacteria can degrade most types of hydrocarbons by utilizing them as energy or carbon sources, although it may take a relatively long time to degrade some recalcitrant compounds [*Atlas*, 1981; *Lee et al.*, 1988].

[3] When organic contaminants from waste disposal sites, leaking chemical storage facilities or accidental spills on the ground surface are introduced into the subsurface environment, the discharged contaminants undergo microbiologic

0043-1397/02/2001WR000344

interactions with indigenous subsurface microorganisms as well as geochemical interactions with aquifer materials. Tightly interlinked with the activity of other microbes such as bacteriophages or fungi, bacterial activities against various types of organic carbon contaminants are observed to be most effective in biodegradation processes in the vadoze zone, especially in the rhizoshpere, which provides a favorable habitat for the bacterial growth with easy accessibility to rich nutrients and moisture [*Atlas*, 1981; *Campbell*, 1983].

[4] When the organic contaminants reach the water table as they migrate downward, they are accumulated on the water table or on the bottom of the saturated aquifer, depending on the density of contaminants. The accumulated contaminants are dissolved into groundwater and widely spread along with groundwater flow. The fate and transport of organic contaminants in the saturated aquifer are affected by advection, dispersion, sorption and biodegradation. The population and activity of bacteria in subsurface soils and groundwater depend on environmental determinants, mainly, the depth at which they live. Studies on the bacterial ecology at depths deeper than the vadose zone indicate that the microbial population decreases considerably as the depth increases. Besides, indigenous bacteria in deep soils often stay in a resting state due to oligotrophic conditions which limit bacterial activities. When natural biodegradation under oligotrophic conditions is not enough to remediate a contaminated aquifer, the efficiency of indigenous bacteria to degrade organic contaminants can be enhanced by adding nutrients required for the biodegradation process [*Semprini et al.*, 1991; *Norris*, 1994; *Flathman et al.*, 1994; *Huesemann and Truex*, 1996]. The rate of overall remediation can be further enhanced by introducing exogenous bacteria which are cultured to treat specific contaminants [*Mayotte et al.*, 1996; *Duba et al.*, 1996]. While introduction of external supply of microbes and/or nutrients, the operation-induced limitations such as excessive biomass accumulation and biocolloid-facilitated transport may affect the efficiency of enhanced bioremediations. As a predictive tool, therefore, bioremediation models should incorporate hydrogeological processes which can affect physical properties of porous media as well as microbial degrading processes.

[5] Although a comprehensive understanding on the fate and transport of microbes as well as contaminants is required to establish effective bioaugmentation strategies, mathematical modeling studies on biodegradation have often focused on bioreactions between organic contaminants and biodegrading bacteria attached to soils [*Molz et al.*, 1986; *Widdowson et al.*, 1988; *Kindred and Celia*, 1989; *Semprini and McCarty*, 1991; *Chen et al.*, 1992; *Zysset et al.*, 1994]. These models stem from experimental observations that most bacteria in saturated aquifers under natural, mostly oligotrophic, conditions appear to be attached to soil particles [e.g., *Harvey et al.*, 1984; *Albrechtsen*, 1994]. Accordingly, the models often do not explicitly address the change of bacterial population due to bacterial transport and the biodegradation by suspended bacteria in the aqueous phase. In contaminated, organic-rich aquifer, however, a noticeable amount of bacteria are observed active in the aqueous phase, although most bacteria reside on the soil surface [*Aamand et al.*, 1989; *Harvey and Barber*, 1992; *Godsy et al.*, 1992; *Murphy et al.*, 1997]. Bacteria in the aqueous phase can originate from the release of bacterial conglomerations on soil surfaces by detachment and cell division or the introduction from adjacent environments. Since suspended bacteria, while migrating through saturated aquifers, can affect microbial population in the solid phase and behave as biodegrading agents or biocolloids, the spatial and temporal distribution of bacteria in both the aqueous and solid phases should be considered in biodegradation models [*Murphy et al.*, 1997; *Chilakapati et al.*, 1998]. Especially in bioaugmentative operations which involve the injection of exogenous bacteria into contaminated aquifers, it is critical to estimate the transport and biodegradation of bacteria in both the aqueous and solid phases.

[6] In mathematical models, biomass in the solid phase is represented as simplified bacterial conglomerations with specified configurations such as continuous film or discontinuous patches. Quantified biomass in the solid phase based on the simplifying assumptions, along with aqueous phase bacterial concentration, is employed to estimate the rates of bacterial growth, decay, attachment/detachment and biodegradation. Biomass in the solid phase has been conceptualized in three ways in the literature [*Baveye and Valocchi*, 1989]. The first approach is the ''macroscopic model,'' in which biomass is assumed as a fully penetrated entity attached to soil surfaces with unspecified configuration. No assumption on the microscopic structure or distribution of biomass is explicitly made in the pore-scale [*Corapcioglu and Haridas*, 1985; *Borden and Bedient*, 1986; *Kindred and Celia*, 1989; *Zysset et al.*, 1994]. The bacterial utilization of contaminants is considered as a macroscopic sink term in mass balance equations, and the aqueous phase concentrations of nutrients and/or contaminants are assumed to limit the bacterial growth. While the macroscopic model has been favored because of its simplicity, it disregards effects of the bacterial growth and spatial distribution of biomass on the hydrologic characteristics in a porous medium. In contrast to the macroscopic model, the ''biofilm model'' and the ''microcolony model'' assume certain configurations of biomass in the solid phase. In the biofilm model, biomass is assumed to cover soil surfaces as a continuous biofilm with a uniform thickness in which the biodegradation process takes place [*Rittman and McCarty*, 1980; *Taylor and Jaffé*, 1990; *Kim and Corapcioglu*, 1996]. In the microcolony model, biomass is assumed to exist in tiny disk-shaped microcolonies scattered over the soil surface, and the change in biomass in the solid phase is considered as a change in the number of microcolonies per unit mass of porous medium [*Molz et al.*, 1986; *Widdowson et al.*, 1988; *Chen et al.*, 1992; *Gallo and Manzini*, 1998]. In both biofilm and microcolony approaches a diffusion limitation between the bulk liquid and biomass is assumed in the mass transfer of dissolved species. Although the biophase configuration is strongly site-specific and little experimental information is available to determine which model is more appropriate in biodegradation modeling, several experimental observations reported that bacterial cells are aggregated into loosely packed colonies rather than continuous uniform films and that the microcolonies are composed of 10–100 bacteria scattered on soil surfaces [*Campbell*, 1983; *Harvey et al.*, 1984; *Vandevivere and Baveye*, 1992]. In addition, the experiments by *Ogram et al.* [1985] implicitly invoked

considerations of the existence of bare soil surface (not covered with bacteria) by demonstrating that the contaminant sorption to the solid matrix greatly reduces the bioavailability of the contaminant.

[7] One of the major difficulties during in situ bioremediation is the permeability reduction due to biomass accumulation, which occurs in bioaugmentation when nutrients and/or bacteria are injected into a contaminated aquifer. The rapid bacterial growth in a rich nutrient condition and the strong attachment of bacteria to soils lead to massive biomass accumulation in pore spaces around injection wells. As the accumulation proceeds, the permeability reduction is getting severe, which makes the injection pressure increase or the injection rate decrease. Finally, the injected solutions are trapped within the wells and the low permeability zone affect surrounding groundwater flow field and distributions of involving chemical species and biodegrading microorganisms. *Semprini et al.* [1991] and *Peyton* [1996] proposed a pulsed nutrient injection strategy to mitigate microbial accumulation problems near injection wells. Conversely, *Duba et al.* [1996] conducted field experiments to take advantage of the bacterial accumulation by adding bacteria and nutrients and constructing a fixed-bed biobarrier. Both cases showed that biomass accumulation can cause reduction in permeability and affect the efficiency of the bioremediation process.

[8] Bacteria, as biosorbents and biodegrading agents, can affect the fate and transport of organic contaminants in the subsurface. Experimental observations have revealed that contaminants can migrate to distances further than predicted by conventional transport models when colloids are present in the subsurface environments [*Magee et al.*, 1991; *Corapcioglu and Jiang*, 1993]. Because most bacteria are colloidal in size ($0.5 \sim 1$ μm) and indigenous in soil and groundwater, they undergo transport patterns similar to colloidal particles in the subsurface [*Alexander*, 1977]. While indigenous or exogenous bacteria migrate in porous media, hydrophobic contaminants dissolved in groundwater can easily adsorb on bacterial surfaces, and their spatial distribution can be altered by bacteria in both the aqueous and solid phases [*Jenkins and Lion*, 1993; *Kim and Corapcioglu*, 1996].

[9] In this study, we propose a two-dimensional mathematical model to investigate the effects of bacterial mobility on the fate and migration of an organic contaminant in bioaugmentation operations. The microcolony approach is applied to conceptualize the bacterial configuration in the solid phase and to estimate the effects of bacterial accumulation on changes in hydrologic properties in a contaminated aquifer. We consider the effects of bacteria as biosorbents as well as biodegrading agents. In the proposed model, a system of coupled mass balance equations for an organic contaminant which is biodegraded through aerobic cometabolism, a primary substrate, an electron acceptor, and bacteria in both the aqueous and solid phases are solved using a fully implicit finite difference method and the altering direction iteration (ADI) scheme. Model comparison is performed against an independently developed model with similar objectives to show the model output robustness. The proposed model is also applied to a numerical experiment on a bioaugmentation using an in situ biobarrier to demonstrate the behavior and applicability of the model and to propose effective bioremediation strategies.

2. Model Development

[10] In this mathematical study, the modeling system for the fate and transport of dissolved species and suspended microbes is restricted to a two-dimensional saturated flow field. Biologically mediated processes such as reproduction, growth and decay are incorporated in mathematical formulations along with physical transport processes. Nutrients for subsurface microorganisms, a primary substrate and an electron acceptor in this model, are considered as limiting components for microbial activities such as biomass growth and biodegradation. Anaerobic degradation may take place after the depletion of oxygen and affect significantly the fate of organic contaminants. However, for the purpose of this study, the proposed model was designed to focus on the biodegradation of a contaminant through aerobic cometabolism. The effects of environmental factors such as pH, temperature, moisture content, etc. on microbial activities are not explicitly considered in model formulations.

2.1. Fate and Transport of Bacteria in Porous Media

[11] The fate and transport of bacteria in the subsurface can be represented by phenomena in the aqueous and solid phases. While advective and dispersive processes dominate bacterial transport in the aqueous phase, the bacteria are attached to and accumulate on soil surfaces in the solid phase. During the migration and accumulation, bacteria also undergo microbiologic processes of reproduction, maintenance, and decay in both the aqueous and the solid phase. The mass balance equation for bacteria in the aqueous phase in saturated porous media can be expressed as

$$\frac{\partial \theta C_c}{\partial t} = -\nabla \cdot \mathbf{J}_c^f - Q_c^s + Q_c^g - Q_c^d \tag{1}$$

where C_c is the mass concentration of bacteria in the aqueous phase [M/L^3] and θ is the water content. Note that $\theta = n - \sigma_c$ in a saturated porous medium, where n is the porosity and σ_c is the volumetric fraction of attached bacteria on the solid matrix (volume of attached bacteria per unit total volume of porous medium). $\mathbf{J}_c^f$ is the specific mass discharge vector of bacteria in the aqueous phase [M/L^{2}T], and Q_c^s is the net rate of bacterial capture on the solid matrix [M/L^{3}T]. Q_c^g and Q_c^d are the rates of bacterial growth and decay, respectively, in the aqueous phase [M/L^{3}T]. If the interstitial velocity of bacteria is assumed to be the same as that of groundwater flow, $\mathbf{J}_c^f$ is expressed as

$$\mathbf{J}_c^f = -\mathbf{D}_c^* \cdot \nabla[\theta C_c] + \mathbf{q}_w C_c \tag{2}$$

where $\mathbf{D}_c^*$ is the hydrodynamic dispersion coefficient tensor for mobile bacteria [L^2/T] and $\mathbf{q}_w$ is the specific discharge vector of groundwater flux [L/T]. Since both $\mathbf{D}_c^*$ and $\mathbf{q}_w$ are functions of the permeability of a porous medium, the value of $\mathbf{J}_i^f$ varies depending on the biomass accumulation on the solid matrix and the permeability change.

[12] While migrating through subsurface porous media by advective-dispersive processes, microbes undergo physical partitioning between the aqueous and solid phase. Microbial

attachment to the solid matrix is caused by Brownian, London-van der Waals, and/or electrostatic forces, while detachment is caused by shear force or change of ionic strength. For a further review on the processes, the reader is referred to *McDowell-Boyer et al.* [1986] and *Corapcioglu and Baehr* [1987]. If the rate of bacterial attachment/detachment is reversible, the net rate of bacterial capture on the solid matrix, Q_c^s, can be expressed as a quasi-empirical first-order kinetic process [e.g., *Corapcioglu and Haridas*, 1985; *Hornberger et al.*, 1992; *Murphy et al.*, 1997].

$$Q_c^s = k_1 \theta C_c - k_2 N_c m_c \tag{3}$$

where k_1 and k_2 are the bacterial attachment and detachment rate coefficients on/from the solid matrix, respectively [1/T], N_c is the microcolony density (number of microcolonies per unit volume of aquifer) [#/L^3], and m_c is the mass of a microcolony [M] which is calculated by $m_c = \rho_c \cdot \pi r_c^2 \tau$ where ρ_c is the density of a microcolony, and r_c and τ are the radius and the thickness of a disk-shaped microcolony, respectively [*Molz et al.*, 1986].

[13] The utilization of organic or inorganic compounds by microorganisms has been represented in several ways such as an instantaneous reaction [*Corapcioglu and Baehr*, 1987; *Rifai and Bedient*, 1990] or as a first-order reaction [*Zysset et al.*, 1994; *McNab and Narasimhan*, 1994]. Among them, the Monod kinetics has been the most widely used to describe the utilization rate of components required in metabolic processes and, thereby, the bacterial growth rate as a function of concentrations of limiting components [*Widdowson et al.*, 1988; *Chen et al.*, 1992; *Semprini and McCarty*, 1992]. The Monod kinetics can be modified to take into account the effect of threshold concentrations or multiple limiting components. If the supplies of a primary substrate and an electron acceptor are considered to limit the bacterial metabolism, the rate of bacterial growth in the aqueous phase, Q_c^g, can be described by multiple Monod kinetics as

$$Q_c^g = \mu_m(C_P, C_O)\left[\frac{C_P}{K_P + C_P}\right]\left[\frac{C_O}{K_O + C_O}\right] \cdot \theta C_c \tag{4}$$

$$\mu_m(C_P, C_O) = \frac{\mu_{max}}{4}\left[1 + \frac{C_P - C_P^T}{|C_P - C_P^T|}\right]\left[1 + \frac{C_O - C_O^T}{|C_O - C_O^T|}\right] \tag{5}$$

where $\mu_m(C_P, C_O)$ is the bacterial growth rate function in the aqueous phase [1/T] and μ_{max} is the maximum specific growth rate of bacteria [1/T]. C_P and C_O are the aqueous phase concentrations of dissolved primary substrate and electron acceptor [M/L^3], respectively. C_P^T and C_O^T are the threshold concentrations of primary substrate and electron acceptor for bacterial growth [M/L^3], respectively. K_P and K_O are the half-saturation constants for primary substrate and electron acceptor, respectively, which are also the concentrations of primary substrate and electron acceptor at 0.5 μ_{max} [M/L^3]. The bacterial growth rate function $\mu_m(C_P, C_O)$ in (5) represents the growth rate as a function of the aqueous phase and threshold concentrations of limiting components; $\mu_m(C_P, C_O) = \mu_{max}$ when $C_P \geq C_P^T$ and $C_O \geq C_O^T$; otherwise $\mu_m(C_P, C_O) = 0$ [*Reddy and Ford*, 1996].

[14] Like other living creatures, bacteria are born, grow, mature, and die. After they die, the carbohydrates, amino acids, and other components are freed from the lysed cells and consumed as nutrients by neighboring active bacteria. Although the lysis of entire cell body may take a considerable amount of time and some recalcitrant part of the cells can remain without breaking down, the entire process is still unclear and strongly dependent on surrounding environments. In the proposed model, therefore, it is assumed that the lysing process is very fast and the dead cells lose their function and volume immediately. If the bacterial decay is a first-order kinetic process, the rate of bacterial inactivation can be expressed as

$$Q_c^d = k_d \theta C_c \tag{6}$$

where k_d is the bacterial decay rate coefficient [1/T]. Substitution of (2)–(6) into (1) yields a mass balance equation for bacteria in the aqueous phase as

$$\frac{\partial \theta C_c}{\partial t} = \nabla \cdot (\mathbf{D}_c^* \cdot \nabla[\theta C_c] - \mathbf{q}_w C_c) - k_1 \theta C_c + k_2 N_c m_c + \mu_m(C_P, C_O)\left[\frac{C_P}{K_P + C_P}\right]\left[\frac{C_O}{K_O + C_O}\right] \cdot \theta C_c + k_d \theta C_c \tag{7}$$

[15] Bacteria in the solid phase also undergo growth and decay in microcolonies. In the microcolony model, the change of biomass in the solid phase is expressed in terms of a microcolony density, N_c [*Molz et al.*, 1986; *Widdowson et al.*, 1988]. If the parameters for bacterial growth and decay, μ_{max}, K_P, K_O and k_d, are assumed to apply to both the aqueous and solid phases [*Corapcioglu and Haridas*, 1985], the mass balance equation for bacteria in the solid phase can be represented as

$$\frac{\partial N_c}{\partial t} = \mu_m(C_{Pc}, C_{Oc})\left[\frac{C_{Pc}}{K_P + C_{Pc}}\right]\left[\frac{C_{Oc}}{K_O + C_{Oc}}\right] N_c - k_d N_c + \frac{k_1 \theta C_c}{m_c} - k_2 N_c \tag{8}$$

where C_{Pc} and C_{Oc} are the concentrations of a primary substrate and an electron acceptor within the microcolony [M/L^3], respectively. The four terms on right–hand side of (8) respectively represent bacterial growth, decay, attachment and detachment in terms of number of microcolonies.

2.2. Fate and Transport of Dissolved Components in Porous Media

[16] During the migration through saturated porous media along with groundwater flow, each dissolved species undergoes similar patterns of reactions with surrounding environments. The mass balance equation representing the fate and transport of dissolved component i in the aqueous phase in saturated porous media can be expressed as

$$\frac{\partial \theta C_i}{\partial t} = -\nabla \cdot \mathbf{J}_i^f - Q_i^s - {}_i^{bio} - Q_i^{mc} - Q_i^{mb} - Q_i^{cb} \tag{9}$$

where subscript i denotes a primary substrate as P, a contaminant as D, and an electron acceptor as O. C_i is the mass concentration of component i dissolved in the aqueous phase [M/L^3]. $\mathbf{J}_i^f$ is the specific mass discharge vector of component i in the aqueous phase [M/L^{2}T]. Q_i^s, Q_i^{bio}, Q_i^{mc},

Q_i^{mb}, and Q_i^{cb} are sink terms for component i [M/L^{3}T], which are the net rate of sorption on the solid matrix, the rate of utilization by suspended bacteria, the rate of mass transfer into microcolonies, and the net rates of biosorption to suspended bacteria in the aqueous phase and attached bacteria in the microcolony, respectively.

[17] The first term on the right-hand side of (9) represents the advective and dispersive flux of component i in the aqueous phase. The specific mass discharge vector of component i, $\mathbf{J}_i^f$, is expressed as

$$\mathbf{J}_i^f = -\mathbf{D}_i^* \cdot \nabla[\theta C_i] + \mathbf{q}_w C_i \tag{10}$$

where $\mathbf{D}_i^*$ is the hydrodynamic dispersion coefficient tensor of component i [L^2/T]. The hydrodynamic dispersion coefficient tensors of bacteria and a dissolved component i, $\mathbf{D}_c^*$ and $\mathbf{D}_i^*$, respectively, are not necessarily the same because of the difference in their molecular diffusion coefficients. In most highly advective systems, however, the difference is neglected and it is assumed that $\mathbf{D}_c^* = \mathbf{D}_i^*$ [*Corapcioglu and Jiang*, 1993].

[18] The second term in (9) represents the net rate of sorption of component i to the solid matrix. If the mass transfer of component i between the aqueous and solid phases is linear and can be represented by an equilibrium adsorption isotherm, the net rate of sorption on the solid matrix, Q_i^s, can be expressed in terms of the aqueous phase concentration of component i, C_i, as

$$Q_i^s = \frac{\partial}{\partial t}(\rho_b \cdot K_{3i} C_i) \tag{11}$$

where ρ_b is the dry bulk density of soils [M/L^3] and K_{3i} is the equilibrium distribution coefficient of dissolved component i with the solid matrix [L^3/M].

[19] The rate of utilization of component i by suspended bacteria is determined by the role of component i in the biodegradation processes. As an electron donor for redox reactions and a carbon source for synthesis of new biomass, heterotrophic bacteria should utilize external organic materials. If the primary substrate is the sole growth substrate, i.e., a secondary substrate, an organic contaminant here, is a nongrowth substrate, the net rate of primary substrate utilization is expressed by multiple Monod kinetics as a function of aqueous concentrations of a primary substrate and an electron acceptor:

$$Q_P^{bio} = \frac{\mu_m(C_P, C_O)}{Y_P}\left[\frac{C_P}{K_P + C_P}\right]\left[\frac{C_O}{K_O + C_O}\right] \cdot \theta C_c \tag{12}$$

where Y_P is the yield coefficient of bacteria for utilizing primary substrate (mass of bacteria per unit mass of utilized primary substrate) [M/M].

[20] Since the contaminant is a nongrowth substrate and biodegradable by bacteria during the metabolism of a primary substrate and an electron acceptor, the rate of transformation of the cometabolic contaminant can be represented to be proportional to the rate of bacterial growth as

$$Q_D^{bio} = \frac{\mu_m(C_P, C_O)}{Y_D}\left[\frac{C_D}{K_D + C_D}\right]\left[\frac{C_P}{K_P + C_P}\right]\left[\frac{C_O}{K_O + C_O}\right] \cdot \theta C_c \tag{13}$$

where Y_D is the yield coefficient of bacteria for a transforming contaminant (mass of bacteria per unit mass of a transformed contaminant) [M/M].

[21] The consumption of electron acceptors is necessary for bacteria to release energy for synthesis and cell maintenance. Therefore the rate of electron acceptor utilization is assumed as a sum of the two needs which are proportional to the rates of bacterial growth and decay, respectively [*Molz et al.*, 1986; *Gallo and Manzini*, 1998]:

$$Q_O^{bio} = \left[\left[\gamma_P + \gamma_D\left[\frac{C_D}{K_D + C_D}\right]\right] \cdot \mu_m(C_P, C_O)\left[\frac{C_P}{K_P + C_P}\right]\left[\frac{C_O}{K_O + C_O}\right] + \alpha k_d\left[\frac{C_O}{K_O' + C_O}\right]\right] \cdot \theta C_c \tag{14}$$

where γ_P and γ_D are the electron acceptor use coefficients for synthesis of a primary substrate and a contaminant [M/M], respectively. α is the electron acceptor use coefficient for cell maintenance, and K_O' is the saturation constant of an electron acceptor for bacterial inactivation [M/L^3].

[22] In (3)–(6), it is assumed that bacteria can utilize only dissolved components in the aqueous phase; in other words, substrates and an electron acceptor sorbed to soils or bacterial surface are not available for bacterial uptake. Although only a few studies reported the biodegradation of sorbed contaminants [*Crocker et al.*, 1995], the assumption has been asserted by several experiments [*Ogram et al.*, 1985; *Alvarez-Cohen et al.*, 1993]. Also, *van Loosdrecht et al.* [1990] described the effect of sorption of contaminants on bioavailability with a geometrical analysis and confirmed the assumption.

[23] The net rates of biosorption for component i to mobile and captured bacteria, Q_i^{mb} and Q_i^{cb}, can be derived from the mass balance equations for component i adhered to surfaces of mobile and captured bacteria, respectively, as [*Kim and Corapcioglu*, 1996]

$$\frac{\partial \theta C_c \sigma_{cm}^i}{\partial t} = Q_i^{mb} - \nabla \cdot \left(\mathbf{J}_c^f \sigma_{cm}^i\right) - k_1 \theta C_c \sigma_{cm}^i + \frac{k_2 N_c m_c}{\theta}\sigma_{cm}^i \tag{15}$$

$$\frac{\partial \theta C_c \sigma_{cc}^i}{\partial t} = Q_i^{cb} + k_1 \theta C_c \sigma_{cm}^i - \frac{k_2 N_c m_c}{\theta}\sigma_{cm}^i \tag{16}$$

where σ_{cm}^i and σ_{cc}^i are the respective mass fractions of component i adhered to bacterial surfaces in the aqueous phase and within the microcolony (mass of adhered component i per unit mass of bacteria) [M/M]. If the biosorption of component i to bacteria is reversible [*Jenkins and Lion*, 1993] and describable by a linear isotherm, though the surface hydrophobicity varies with neighboring nutrient conditions [*Bengtsson et al.*, 1993], σ_{cm}^i and σ_{cm}^i can be expressed in terms of C_i as

$$\sigma_{cc}^i = K_{4i} C_i; \quad \sigma_{cm}^i = K_{5i} C_i \tag{17}$$

where K_{4i} and K_{5i} are the equilibrium distribution coefficients of dissolved component i with captured and suspended bacteria [L^3/M], respectively. Since bacteria in the aqueous phase and in the microcolony have similar surface characteristics [*van Loosdrecht et al.*, 1990], identical distribution coefficients, i.e., $K_{4i} = K_{5i}$, can be

assumed. Like colloidal particles, bacteria are a very effective sorbent to dissolved components such as organic hydrocarbon contaminants in the aqueous phase [*Bengtsson et al.*, 1993]. The rate of contaminant biosorption on bacterial surfaces is much greater than the rate of change in contaminant concentration due to other processes such as advective flow. Therefore the biosorption may reduce the bioavailability of contaminants by reducing the aqueous phase contaminant concentration [*Ogram et al.*, 1985]. The net rate of electron acceptor biosorption to mobile and captured bacteria is often neglected because of its low sorption rate.

[24] The mass transfer of component i from the aqueous phase into microcolonies is assumed to take place through a diffusive boundary layer with a thickness of δ [*Molz et al.*, 1986; *Widdowson et al.*, 1988]. Because the boundary layer is very thin, the diffusive mass transfer across the layer is very fast compared to concentration changes in the aqueous phase, so that a steady state condition, i.e., a constant and uniform concentration gradient, can be assumed across the boundary layer. Therefore the net mass transfer rate of component i from the aqueous phase into microcolonies, Q_i^{mc}, can be expressed as

$$Q_i^{mc} = D_{ib} \cdot N_c \pi r_c^2 \left[\frac{C_i - C_{ic}}{\delta}\right] \tag{18}$$

where D_{ib} is the diffusion coefficient of component i in the diffusive boundary layer [L^2/T] and C_{ic} is the concentration of dissolved component i within the microcolony.

[25] Substitution of (10)–(18) into (9) yields a set of mass balance equations representing the fate and transport of a primary substrate, a cometabolic organic contaminant, and an electron acceptor in the aqueous phase as, respectively,

$$\frac{\partial C_P}{\partial t}\left[1 + \frac{K_{3P}\rho_b}{\theta} + \frac{K_{4P}N_c m_c}{\theta} + K_{5P}C_c\right] = \frac{1}{\theta}\left(\mathbf{J}_P^f + \mathbf{J}_c^f \cdot K_{5P}C_P\right) - \frac{D_{Pb} \cdot N_c \pi r_c^2}{\theta}\left[\frac{C_P - C_{Pc}}{\delta}\right] - \frac{\mu_m(C_P, C_O)}{Y_P}\left[\frac{C_P}{K_P + C_P}\right]\left[\frac{C_O}{K_O + C_O}\right]C_c \tag{19}$$

$$\frac{\partial C_D}{\partial t}\left[1 + \frac{K_{3D}\rho_b}{\theta} + \frac{K_{4D}N_c m_c}{\theta} + K_{5D}C_c\right] = \frac{1}{\theta}\left(\mathbf{J}_D^f + \mathbf{J}_c^f \cdot K_{5D}C_D\right) - \frac{D_{Db} \cdot N_c \pi r_c^2}{\theta}\left[\frac{C_D - C_{Dc}}{\delta}\right] - \frac{\mu_m(C_P, C_O)}{Y_D}\left[\frac{C_D}{K_D + C_D}\right]\left[\frac{C_P}{K_P + C_P}\right]\left[\frac{C_O}{K_O + C_O}\right]C_c \tag{20}$$

$$\frac{\partial C_O}{\partial t}\left[1 + \frac{K_{3O}\rho_b}{\theta} + \frac{K_{4O}N_c m_c}{\theta} + K_{5O}C_c\right] = \frac{1}{\theta}\left(\mathbf{J}_O^f + \mathbf{J}_c^f \cdot K_{5O}C_O\right) - \left[\gamma_P + \gamma_D\left[\frac{C_D}{K_D + C_D}\right]\right] \cdot \mu_m(C_P, C_O)\left[\frac{C_P}{K_P + C_P}\right]\left[\frac{C_O}{K_O + C_O}\right]C_c - \alpha k_d C_c\left[\frac{C_O}{K'_O + C_O}\right] - \frac{D_{Ob} \cdot N_c \pi r_c^2}{\theta}\left[\frac{C_O - C_{Oc}}{\delta}\right] \tag{21}$$

[26] The component i within a microcolony is diffused from the aqueous phase and utilized by captured bacteria in the microcolony for their metabolism. Therefore the concentration of a primary substrate, a contaminant, and an electron acceptor within the microcolony can be calculated from the mass balance equation across the diffusive layer between the aqueous phase and a microcolony as

$$D_{Pb}\left[\frac{C_P - C_{Pc}}{\delta}\right]\pi r_c^2 = \frac{\mu_m(C_{Pc}, C_{Oc})m_c}{Y_P}\left[\frac{C_{Pc}}{K_P + C_{Pc}}\right]\left[\frac{C_{Oc}}{K_O + C_{Oc}}\right] \tag{22}$$

$$D_{Db}\left[\frac{C_D - C_{Dc}}{\delta}\right]\pi r_c^2 = \frac{\mu_m(C_{Pc}, C_{Oc})m_c}{Y_D}\left[\frac{C_{Dc}}{K_D + C_{Dc}}\right] \cdot \left[\frac{C_{Pc}}{K_P + C_{Pc}}\right]\left[\frac{C_{Oc}}{K_O + C_{Oc}}\right] \tag{23}$$

$$D_{Ob}\left[\frac{C_O - C_{Oc}}{\delta}\right]\pi r_c^2 = \left[\gamma_P + \gamma_D\left[\frac{C_{Dc}}{K_D + C_{Dc}}\right]\right] \cdot \mu_m(C_{Pc}, C_{Oc})\left[\frac{C_{Pc}}{K_P + C_{Pc}}\right]\left[\frac{C_{Oc}}{K_O + C_{Oc}}\right] + \alpha k_d m_c\left[\frac{C_{Oc}}{K'_O + C_{Oc}}\right] \tag{24}$$

2.3. Permeability Reduction Due to Bioaccumulation

[27] As the microcolony density increases, the accumulated biomass occludes the pore space, and the permeability of the porous medium decreases. Although various researchers expressed the permeability reduction as a generalized equation in terms of the volumetric fraction of accumulated bacteria, no currently available bioclogging model can satisfactorily predict the permeability and hydraulic conductivity reduction. Started from the Kozeny-Carmen equation, most permeability reduction models had been developed on the basis of simplifying assumptions for pore space geometry and biomass configuration. Despite of differences in defining pore space, they had commonly assumed that solid phase biomass covers soil surface with continuous biofilms [*Ives and Pienvichitr*, 1965; *Taylor and Jaffé*, 1990; *Taylor et al.*, 1990]. The biofilm-based models tend to slightly overestimate the hydraulic conductivity reduction in coarse-textured media and seriously underestimate it in fine-textured media. It is possibly because of their basic simplifying assumptions on biomass accumulation as a continuous biofilm rather than as a large number of tiny loose-packed colonies as well as on pore space [*Vandevivere et al.*, 1995]. Despite such experimental observations of colonized biomass, however, no permeability reduction model based on the microcolony approach has been introduced in the literature, mainly because of the difficulties in representation of randomly accumulated microcolonies in the pore space.

[28] Instead of making any specific assumptions on configurations of biomass accumulation, *Clement et al.* [1996] developed an analytical equation for permeability change due to biomass accumulation based on macroscopic estimates of average biomass concentrations. When the concentrations of dissolved species are low enough not to alter the viscosity and density of bulk groundwater significantly, hydraulic conductivity change is represented as

$$\frac{K_s}{K_{s0}} = \left(1 - \frac{\sigma_c}{n}\right)^{19/6}; \quad \sigma_c = N_c \cdot \pi r_c^2 \tau \tag{25}$$

where K_s is the saturated hydraulic conductivity [L/T] and K_{s0} is the saturated hydraulic conductivity of a clean porous medium [L/T]. Although the *Clement et al.* [1996] model showed similar predictions to biofilm-based models, we employed it for estimating hydraulic conductivity reduction in the proposed model because of its simplicity and its theoretical approach without assumptions of biofilm.

[29] Permeability reduction models introduced so far in the literature provide only limited information on bioclogging. However, even the limited information from these models can be useful in considering effects of the reduced permeability on the transport of contaminants and the entire bioremediation projects.

3. Solutions of Governing Equations

[30] A system of coupled mass balance equations was solved numerically using a fully implicit finite difference method and the ADI scheme. The complete model contains nine governing equations for nine unknowns (C_c, C_P, C_{Pc}, C_D, C_{Dc}, C_O, C_{Oc}, N_c, and σ_c).

[31] In numerical procedures, the bacterial transport equation (7) is solved for C_c at time step $t + 1$ using C_P, C_O and N_c at time step t, where t is the previous time step when all variables are known. C_P, C_D, and C_O at time step $t + 1$ are sequentially solved from mass balance equations for a primary substrate, a contaminant, and an electron acceptor in the aqueous phase (19)–(21), using data at time step t. Then, calculations for aqueous phase concentrations are completed and the results, C_c, C_P, C_D, and C_O, at time step $t + 1$, update those concentrations at time step t. The microcolony density, N_c, in (8) is calculated using updated aqueous phase concentrations, and then, the volume fraction of biomass, σ_c, is obtained from N_c. Finally, the concentrations, C_{Pc}, C_{Dc}, and C_{Oc}, are calculated from mass balance equations for a primary substrate, a contaminant, and an electron acceptor within the microcolony (22)–(24) employing the modified Newton-Raphson method. Before advancing to the next time step, new groundwater flow field is calculated from a steady state flow model using newly obtained hydraulic conductivities over the simulation domain from (25) with respect to the volumetric fraction of attached bacteria on solid matrix σ_c. As a local biomass accumulation proceeds, the permeability reduction gets accelerated exponentially, especially near injection wells. To avoid the divergence of solutions, a time step varying inversely proportional to the biomass accumulation was employed. These calculation processes are repeated during the model simulations. The numerical scheme was validated by examining the mass balance of each component throughout the simulations and by performing the convergence analysis.

4. Model Evaluation and Application

[32] A rigorous validation of a mathematical model would need a comparison of its numerical solutions with analytical solutions or experimental data set with high spatial and temporal resolution. However, due to the complexity of coupled mass balance equations and the large number of model parameters in the proposed system, the model verification against analytical or experimental data is often impossible except in the simplest cases. As an alternative for model evaluation, therefore, we present a comparison of our simulation results against those from an independently developed bioremediation model by *Murphy et al.* [1997] and a feasible model application for simulating a field-scale bioaugmentation involving the introduction of exogenous bacteria along with nutrients into a contaminated aquifer.

4.1. Model Comparison With an Intermediate-Scale Experiment for Aerobic Biodegradation

[33] The influence of physical heterogeneity on the biodegrading process was investigated via experimental and numerical studies at an intermediate-scale by *Murphy et al.* [1997]. In the modeling efforts, they developed a two-dimensional, multicomponent reactive transport model for simulating transport with aerobic biodegradation in the subsurface, which was partially validated with their own experimental data. Despite the similarities in their formulations – both models used a Monod formulation for degrading reactions and first-order kinetic relationship for bacterial attachment/detachment, the two models have a few fundamental differences in model formulation. The proposed model employed a microcolony model for solid phase biomass and considered the change in flow field caused by permeability reduction, while the *Murphy et al.* [1997] model applied a macroscopic model and considered the change in flow field caused by density and viscous change in the bulk solution. Therefore it should be noted that we present the comparison here to show model robustness for essential formulation and numerical calculation procedures only.

[34] The numerical experiment simulates a flow cell ($0.2 \times 0.2 \times 1.0$ m) which is being contaminated by benzoate pulse and performing aerobic biodegradation. Physical heterogeneities were created with low-conductivity inclusions embedded in a high-conductivity sand matrix which was inoculated with *Pseudomonas cepacia sp*. Due to the short period of simulation (7 days), microbial decay and permeability reduction were not considered in the simulation. The model parameters used by *Murphy et al.* [1997] were converted into equivalent values suitable for applying to the proposed model. For further information on the experiments or physical and biological parameters used in these simulations, readers may refer to *Murphy et al.* [1997].

[35] Figure 1 demonstrates the simulated spatial concentration profiles of a substrate (benzoate) and an electron acceptor (oxygen) in the aqueous phase at $t = 84$ hours. Despite fundamental differences between the two models, simulations conducted for the same flow conditions and equivalent rate coefficients, resulting from either model, show a remarkably close match in the concentration profile in both species. This indicates that the model outputs are rather robust and not very sensitive to the alterations in the biophase configurations between a microcolony model and a macroscopic model as *Baveye and Valocchi* [1989] pointed out.

4.2. Simulation Scenario: Screening the Contaminant Plume by an In Situ Biobarrier

[36] A numerical experiment was performed to demonstrate the applicability of the proposed model. The proposed model was applied to simulate a bioaugmentative operation

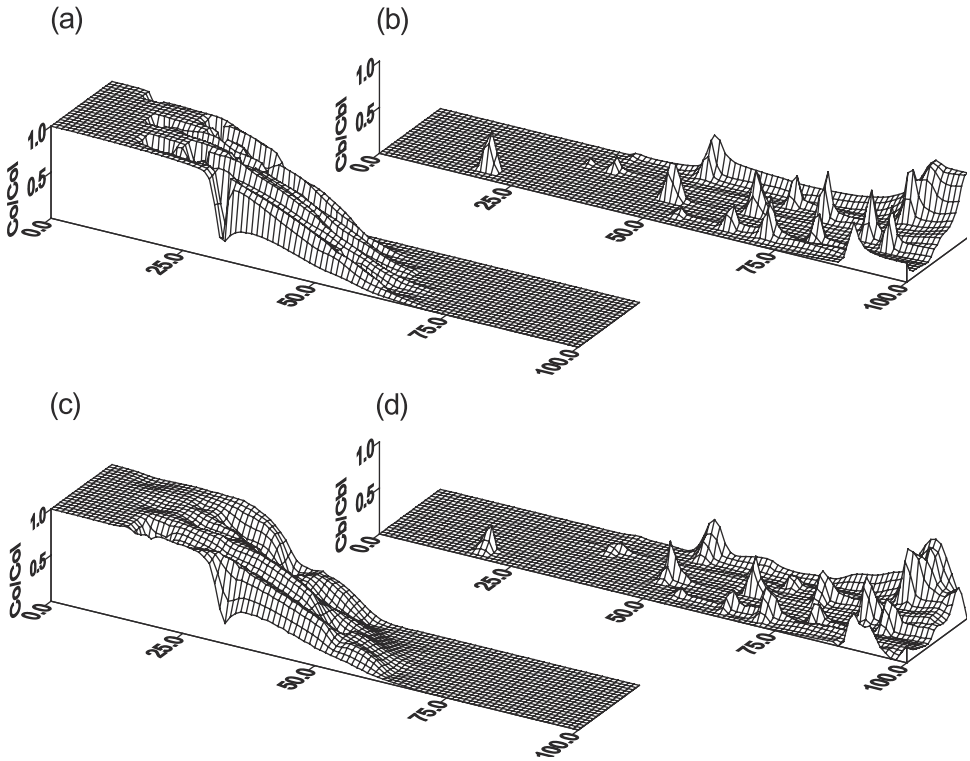

Figure 1. Benzoate and oxygen concentration profiles from (a and b) *Murphy et al.* [1997]'s model and (c and d) the proposed model.

for treating migrating trichloroethylene (TCE) plume using an in situ biobarrier constructed with exogenous methane-oxidizing bacteria. Methane and oxygen were also injected into the contaminated aquifer as a primary substrate and a favorite electron acceptor to enhance the metabolic activities of indigenous and exogenous microorganisms within the biobarrier. To intercept and treat a fast moving contaminant plume, a fixed-bed biobarrier was installed through an injection well for exogenous bacteria ahead of the plume in the direction of groundwater flow. Another well was also installed in the upstream for recharging a solution containing methane and oxygen (Figure 2). TCE is a widespread contaminant in the subsurface and had been commonly used as a solvent in dry cleaning, in degreasing of metal objects, and in extraction processes. Although both aerobic and anaerobic microbes are capable of degrading TCE, it can be mineralized at a relatively higher rate by methanotrophic bacteria via cometabolism under the aerobic condition, which has been widely reported in the literature [*Wilson and Wilson*, 1985; *Oldenhuis et al.*, 1989; *Semprini and McCarty*, 1991; *Semprini et al.*, 1991]. *Duba et al.* [1996] proposed a bioremediation strategy using an in situ microbial barrier constructed with exogenous bacteria and demonstrated its applicability to treat migrating TCE plumes.

[37] Physical configurations for the numerical experiment are depicted on Figure 3. The model domain was 20 × 20 m in the x and y directions represented by 101 × 101 nodes. All sides of the rectangular model domain were set as constant head boundaries to generate a groundwater flow at 1 m/day from left to right under the natural gradient condition. The longitudinal and transverse dispersivities were 0.5 and 0.1 m, respectively. The porosity and the dry bulk density of aquifer material were 0.3 and 1.6 g/cm^3. The initial TCE plume was defined with a constant aqueous concentration of 2 mg/L and low sorption characteristics to soils (K_{3D} = 2 × 10^{-7} L/mg) over the area of 2 m × 2 m at 5 m away from the bacteria injection well (W1). Indigenous bacteria were assumed active on soil surfaces with a microcolony density of 500 cm^{-3}. To stimulate the construction of an in situ biobarrier, groundwater containing exogenous bacteria of strong sorption characteristics to soils (k_1 = 7.0 day^{-1} and k_2 = 0.6 day^{-1}) was injected at the aqueous phase concentration of 100 mg/L through W1 for 16 days. Dissolved methane and

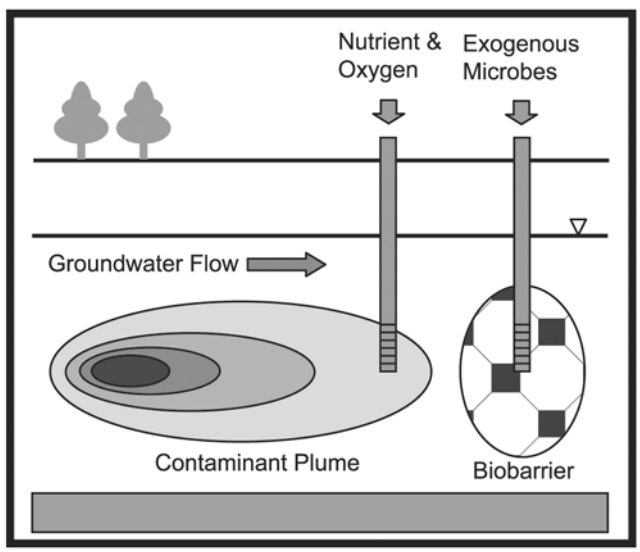

Figure 2. Schematic diagram for bioaugementation using in situ biobarrier.

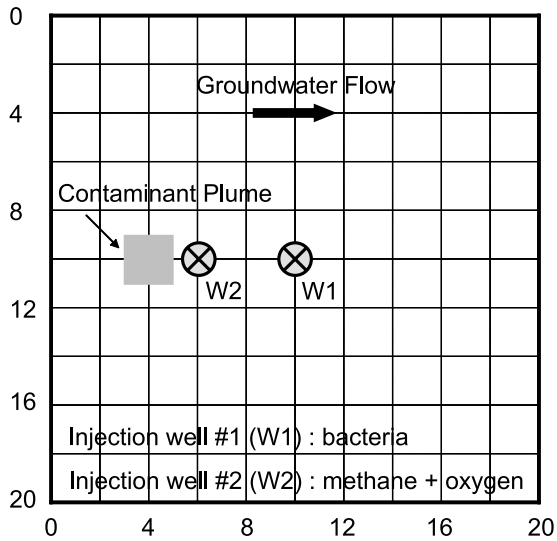

Figure 3. Areal view of model domain in the simulation.

oxygen at respective concentrations of 50 mg/L and 8 mg/L were continuously injected into the aquifer to enhance bacterial activity. Their initial background concentrations were 2 mg/L and 6 mg/L, respectively. The methane and oxygen injection well (W2) was installed at 4 m upstream from W1 to alleviate the excessive biomass growth around W1 and to supply methane and oxygen to a wider area through dispersive spreading. The two injection wells, W1 and W2, and the contaminant plume were placed on a line in the direction of groundwater flow to direct the contaminant plume through the biobarrier. Input concentrations and microbiological and geochemical parameters used in the simulation are summarized in Tables 1 and 2.

[38] Simulated concentration profiles of methane and oxygen in the aqueous phase and the microcolony density at day 4 are shown in Figure 4. Due to strong sorption characteristics, the injected bacteria were rapidly accumulated on the solid matrix around W1 and build up huge numbers of tiny loose-packed microcolonies. Due to the continuous bacterial injection, biomass accumulation was spread toward surroundings, mainly downstream, and an elliptic biobarrier was constructed around W1. While any available nutrients near the biobarrier were rapidly depleted by a large population of bacteria in the aqueous phase and within the microcolony, only limited amounts of methane and oxygen dispersed from surroundings supported natural biodegradation by indigenous bacteria at a relatively low rate in the downstream of the biobarrier. Most of the biodegradation at a higher rate occurred within the biobarrier and in the region between W1 and W2 because of the high bacterial density and the replenishment of methane and oxygen from W2.

[39] Figure 5 illustrates the fate and migration of the TCE plume and the growth of the biobarrier for 16 days after the introduction of exogenous bacteria and nutrients, and Figure 6 shows the distributions of net rate of total TCE biotransformation, which includes biodegradation both in the aqueous phase and within microcolonies, at days 4 and 12. The TCE plume migrated downstream with longitudinal and transversal spreading and passed through the biobarrier with undergoing intrinsic and enhanced biotransformation. When the introduction of exogenous bacteria and the development of biobarrier started, TCE plume was far from the biobarrier and advective-dispersive transport and intrinsic biodegradation controlled the distribution of the contaminant plume. Since indigenous bacteria were degrading TCE in the plume at a relatively low rate, and only a small portion of the plume came in contact with bacteria in the biobarrier, the overall rate of biodegradation in the entire domain was still very low. As the injection of bacteria continued, the biobarrier was fully developed and the TCE plume passed through the biobarrier (the area with high biomass density around two injection wells) (days 4 and 8). The continuous nutrient injection through W2 created rich nutrient conditions around W2 and downstream and stimulated metabolic processes in the area. Due to the TCE biotransformation at a high rate (day 4 in Figure 6), the concentration of TCE was significantly decreasing while the plume was passing through the biobarrier area. As the operation proceeded, (days 12 and 16), untreated TCE plume at a very low concentration passed by the biobarrier, and natural biodegradation by indigenous bacteria barely continued due to the depletion of methane and oxygen at the downstream of the biobarrier (day 16 in Figure 6.) Excessively grown biomass around W2 immediately consumed most of injected nutrients and the microcolony density around W1 started to decrease rapidly without external nutrient supply. Eventually at day 20 (not shown), most of the plume disappeared out of the simulation domain and biodegradation processes become negligible.

[40] Figure 7a shows the relative mass of TCE transformed by biodegradation with and without exogenous bacteria injection, and Figure 7b explains the change of the relative mass of TCE in each phase during the 16-day operation. When methane and oxygen were continuously injected during the entire simulation period, the biodegradation with the addition of exogenous bacteria transformed 31.2% more mass of TCE than that with indigenous bacteria only. In the biobarrier operation involving the injection of bacteria, 67.5% of initial TCE in the aqueous and solid phases was biodegraded by indigenous and exogenous bacteria for the entire simulation period (16 days). More than 74.7% of biodegradation occurred between days 4–12 when the TCE plume was passing through the biobarrier. After day 12, as mentioned earlier, biodegradation rate significantly decreased because of low concentrations of methane and oxygen.

[41] Bacteria can also remove dissolved contaminants from the aqueous phase by providing additional sorption sites. Due to the contact of TCE plume and biobarrier, the amount of TCE sorbed on bacterial surfaces peaked around days 4–8. After then, as aqueous concentration of TCE decreased by transport and biodegradation, the biosorbed

Table 1. Input Concentrations Used in the Simulation

	Background Concentration	Injection Concentration	Threshold Concentration
TCE	0 mg/L	2 mg/L (in TCE plume)	–
Methane	2 mg/L	50 mg/L	0.01 mg/L
Oxygen	6 mg/L	8 mg/L	0.01 mg/L
Suspended bacteria	0 mg/L	200 mg/L	–
Microcolony	500 cm^{-3}	–	–

Table 2. Microbiological and Geochemical Parameters Used in the Simulation

Parameters	Values Used in Simulation	Values Reported in Literature[a]
Microorganisms (bacteria)		
Attachment rate coefficients on the solid matrix	7.0 day^{-1}	1.4 (1) – 180 (2)
Detachment rate coefficients from the solid matrix	0.6 day^{-1}	0.3 (2) – 2.4 (2)
Decay rate coefficient	0.15 day^{-1}	0.1 (3) – 0.549 (4)
Yield coefficient for transforming TCE	0.4	0.426 (4)
Yield coefficient for utilizing methane	0.5	0.5 (5)
Maximum specific growth rate of bacteria	2.0 day^{-1}	2.0 (5) – 4.4 (4)
Contaminant (TCE)		
Equilibrium distribution coefficient with the solid matrix	2.0×10^{-7} L/mg	2.0×10^{-7} (6)
Equilibrium distribution coefficients with captured bacteria	0.01 L/mg	–
Equilibrium distribution coefficients with suspended bacteria	0.01 L/mg	–
Half-saturation constant	2.0 mg/L	0.42 (3) – 1.94 (4)
Substrate (methane)		
Equilibrium distribution coefficient with the solid matrix	0.0 L/mg	0.0 (5)
Equilibrium distribution coefficients with captured bacteria	0.01 L/mg	–
Equilibrium distribution coefficients with suspended bacteria	0.01 L/mg	–
Half-saturation constant	6.0 mg/L	0.03 (3) – 6.85 (4)
Electron acceptor (oxygen)		
Equilibrium distribution coefficient with the solid matrix	0.0 L/mg	0.0 (5)
Equilibrium distribution coefficients with captured bacteria	0.0 L/mg	–
Equilibrium distribution coefficients with suspended bacteria	0.0 L/mg	–
Half-saturation constant	1.0 mg/L	1.0 (5)
Saturation constant for bacterial decay	0.1 mg/L	0.077 (7)
Electron acceptor use coefficient for cell maintenance	0.71	0.04 (7) – 1.42 (5)
Electron acceptor use coefficients for synthesis of TCE	0.5	–
Electron acceptor use coefficients for synthesis of methane	1.2	1.4 (7) – 2.4 (5)
Microcolony		
Radius of a disk-shaped microcolony	0.0005 cm	0.0001 (8) – 0.0005 (7)
Diffusive boundary layer thickness	0.01 cm	0.01 (7)
Density of a microcolony	9.0×10^4 mg/L	$9.0 \times 10^{4(7)}$
Thickness of a disk-shaped microcolony	0.0005 cm	10^{-6} (8) – 0.0005 (7)

[a]Numbers in parentheses refer to the following references: 1, *Murphy et al.* [1997]; 2, *Hornberger et al.* [1992]; 3, *Anderson and McCarty* [1994]; 4, *Chang and Criddle* [1997]; 5, *Semprini and McCarty* [1991]; 6, *Semprini et al.* [1991]; 7, *Molz et al.* [1986]; 8, *Widdowson et al.* [1988].

TCE was readily desorbed back into the aqueous phase. Although the effect of contaminants biosorption to degrading microbes is incorporated in the presented model, we here applied very conservative values for biosorption parameters due to the lack of available data on biosorption between biodegradable contaminants and biodegrading microbes and the effects appeared minimal. It should be noticed that further studies on it need more detailed experimental information.

[42] The hydraulic conductivity reductions due to biomass accumulation at days 4 and 16 are compared in Figure 8. In the early time (day 4) when the continuously injected bacteria spread into the aquifer and constructed a biobarrier, the strong sorption characteristics of bacteria resulted in a high density of microcolony and the hydraulic conductivity reduction around W1. As the bacteria injection continued, the biobarrier expanded into an elliptic shape due to the bacterial migration toward the downstream. While biomass accumulation around W1 resulted mainly from the strong sorption characteristics, rich nutrient conditions created by nutrients injection caused the biomass accumulation around W2. An accelerated bacterial growth caused permeability and hydraulic conductivity reduction up to 90% near W2. Although only a limited region around injection wells was affected by serious hydraulic conductivity reduction, a broader biobarrier region experienced a certain degree of reduction, which had opposite effects on bioaugmentation. The local permeability reduction affected the surrounding flow field, which governed the transport and distribution of nutrients, degrading microbes and contaminants, to bypass the biobarrier region. On the other hand, slow groundwater flow induced by permeability reduction increased residence time of dissolved contaminants entered into the biobarrier region and enhanced the remediation efficiency of recalcitrant contaminants. Despite continuous bacterial injection, therefore, the microcolony density around W1 does not increase significantly due to bacterial decay and migration compensating bacterial growth at a low rate in oligotrophic conditions (day 16).

5. Conclusions

[43] This study presents a two-dimensional mathematical model for simulating the fate and transport of an organic contaminant through cometabolism during the in situ bioaugmentation in saturated porous media. Enhanced biodegradation resulting from the introduction of exogenous microbes and nutrients was simulated and coupled with dynamic transport of biomass and biomass accumulation under varying groundwater flow conditions. A microcolony model was applied to represent the biomass configuration in the solid phase. The effect of local permeability reduction caused by biomass accumulation on biodegradation process was investigated. The role of bacteria as biosorbents was incorporated in model formulations. A system of mass balance equations of a primary substrate, an electron acceptor, biomass and cometabolic contaminant of interest coupled with one another via geochemical and biotic reaction terms are constructed and solved numerically using a finite-different approximation and the ADI scheme.

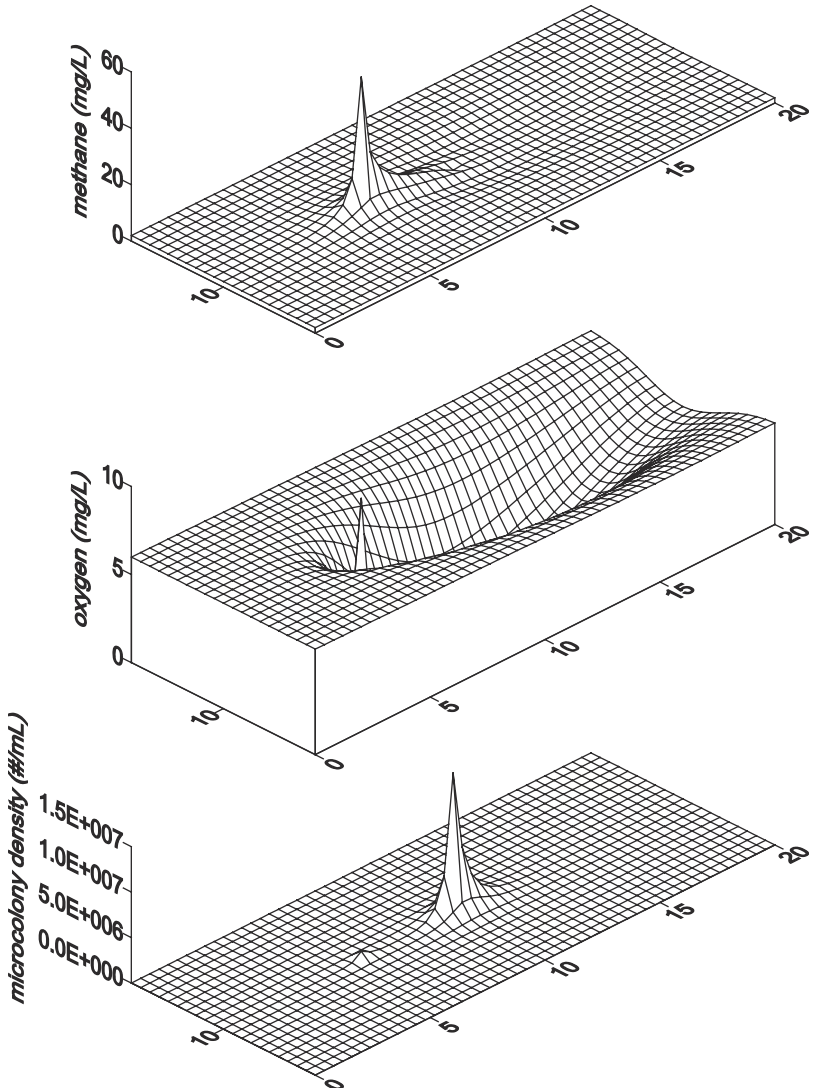

Figure 4. Areal aqueous phase concentrations of methane and oxygen and microcolony density at day 4.

[44] For the evaluation purpose, a model comparison was performed against an existing mathematical model which was independently developed, partially validated by *Murphy et al.* [1997]. Despite a few fundamental differences, simulations conducted for the same flow conditions and equivalent rate coefficients, resulting from either model, showed remarkably close matches in the concentration profiles of the substrate and electron acceptor. In addition to the robustness, it indicates that the model outputs are not very sensitive to the alterations in the biophase configurations between a microcolony model and a macroscopic model.

[45] In the presented numerical experiments, we have shown that the bioaugmentative operations have significant effects on the fate and distribution of all the chemical species and biomass simulated and how these components may interact. Enhanced efficiency of bioaugmentation resulting from the introduction of exogenous microbes and nutrients was demonstrated. Also, it is noted that the efficiency can be adversely affected by operation-induced limitations such as permeability reduction. Obviously, simulation results confirmed that the biodegradation rate determined by the distribution of biomass and the bioavailability of required nutrients. These results implied that the success of in situ bioaugmentation depends on how to control the contact of biodegrading microbes with contaminants and how to supply enough nutrients into the contaminated zone and stimulate microbial activities.

Notation

C_c mass concentration of bacteria in the aqueous phase [M/L^3].

C_i mass concentration of component i dissolved in the aqueous phase [M/L^3].

C_{ic} concentration of dissolved component i within the microcolony [M/L^3].

C_P^T, C_O^T threshold concentrations of primary substrate and electron acceptor for bacterial growth [M/L^3].

C_{Pc}, C_{Oc} concentrations of a primary substrate and an electron acceptor within the microcolony [M/L^3].

$\mathbf{D}_c^*$ hydrodynamic dispersion coefficient tensor for mobile bacteria [L^2/T].

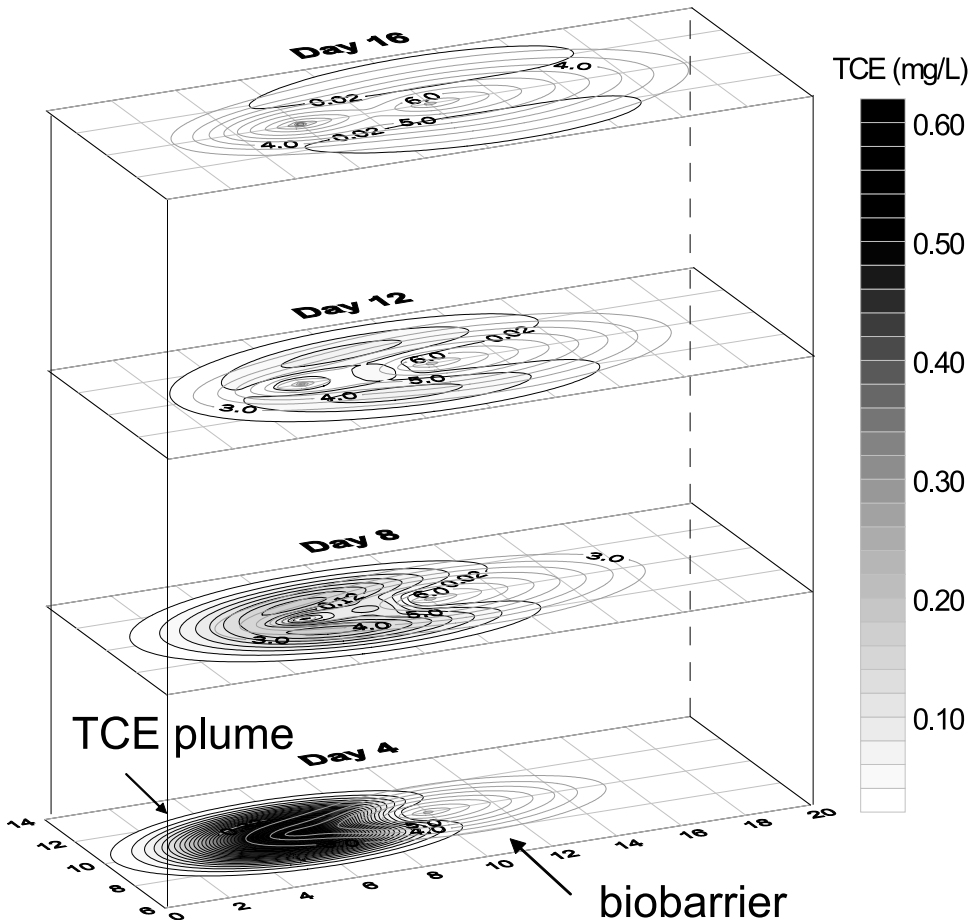

Figure 5. The fate of transport of TCE plume passing through the in situ biobarrier. Microcolony density in biobarrier area is represented by logarithmic equidensity lines, starting with 3.0 ($N_c = 10^3$ cm^{-3}) and increasing by 0.5.

$\mathbf{D}_i^*$ hydrodynamic dispersion coefficient tensor of component i [L^2/T].
D_{ib} diffusion coefficient of component i in the diffusive boundary layer [L^2/T].
$\mathbf{J}_c^f$ specific mass discharge vector of bacteria in the aqueous phase [M/L^2T].
$\mathbf{J}_i^f$ specific mass discharge vector of component i in the aqueous phase [M/L^2T].
k_1, k_2 bacterial attachment and detachment rate coefficients on/from the solid matrix [1/T].
K_{3i} equilibrium distribution coefficient of dissolved component i with the solid matrix [L^3/M].
K_{4i}, K_{5i} equilibrium distribution coefficients of dissolved component i with captured and suspended bacteria [L^3/M].
K_s saturated hydraulic conductivity [L/T].
K_{s0} saturated hydraulic conductivity of a clean porous medium [L/T].
K'_O saturation constant of an electron acceptor for bacterial decay [M/L^3].
K_P, K_O half-saturation constants for primary substrate and electron acceptor [M/L^3].
k_d bacterial decay rate coefficient [1/T].
m_c mass of a microcolony [M].
N_c microcolony density (number of microcolonies per unit volume of aquifer) [number/L^3].

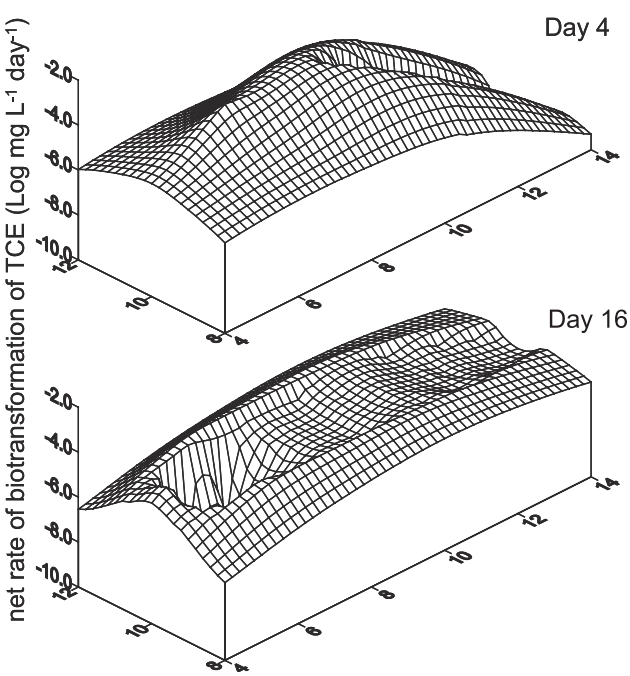

Figure 6. The net rate of total TCE biotransformation at days 4 and 16.

n porosity.

Q_c^g, Q_c^d rates of bacterial growth and decay, respectively, in the aqueous phase [M/L^{3}T].

Q_c^s net rate of bacterial capture on the solid matrix [M/L^{3}T].

Q_i^s net rate of sorption of component i on the solid matrix [M/L^{3}T].

Q_i^{bio} net rate of utilization of component i by suspended bacteria [M/L^{3}T].

Q_i^{mb}, Q_i^{cb} net rates of biosorption for component i to mobile and captured bacteria [M/L^{3}T].

Q_i^{mc} net mass transfer rate of component i from the aqueous phase into microcolonies [M/L^{3}T].

$\mathbf{q}_w$ specific discharge vector of groundwater flux [L/T].

r_c, τ radius and the thickness of a disk-shaped microcolony [L].

Y_D yield coefficient of bacteria for a transforming contaminant (mass of bacteria per unit mass of a transformed contaminant) [M/M].

Y_P yield coefficient of bacteria for utilizing primary substrate (mass of bacteria per unit mass of utilized primary substrate) [M/M].

α electron acceptor use coefficient for cell maintenance.

γ_P, γ_D electron acceptor use coefficients for synthesis of a primary substrate and a contaminant [M/M].

θ water content.

$\mu_m(C_P, C_O)$ bacterial growth rate function in the aqueous phase [1/T].

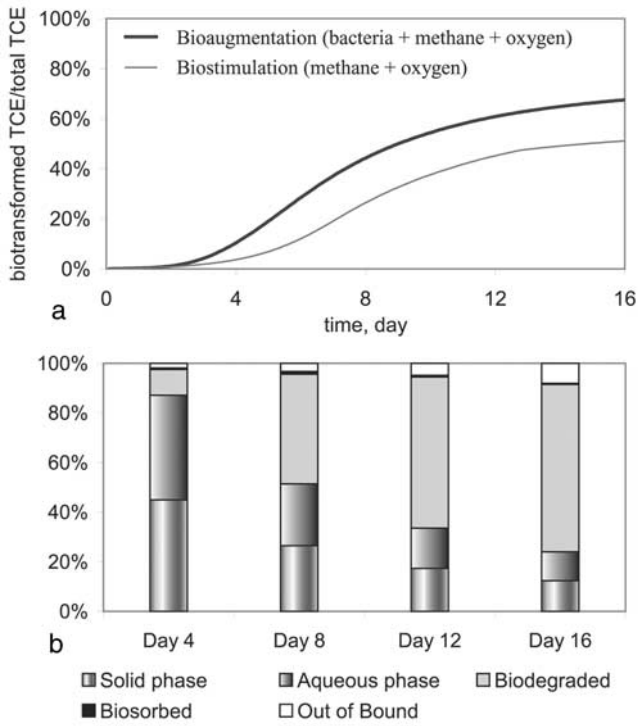

Figure 7. (a) The relative mass of TCE transformed by biodegradation with and without exogenous bacteria injection, and (b) the change of the relative mass of TCE in each phase with exogenous bacteria injection.

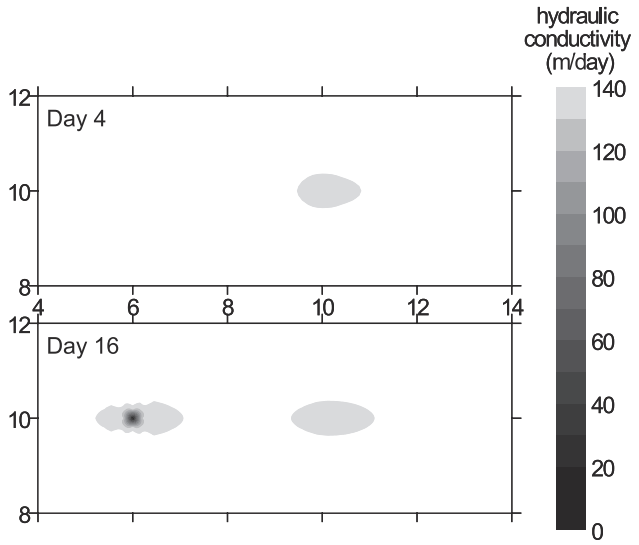

Figure 8. The hydraulic conductivity reduction due to biomass accumulation at days 4 and 16.

μ_{max} maximum specific growth rate of bacteria [1/T].

ρ_b dry bulk density of soils [M/L^3].

ρ_c density of a microcolony.

σ_c volumetric fraction of attached bacteria on the solid matrix (volume of attached bacteria per unit total volume of porous medium) [V/V].

σ_{cm}^i, σ_{cc}^i mass fractions of component i adhered to bacterial surfaces in the aqueous phase and within the microcolony (mass of adhered component i per unit mass of bacteria) [M/M].

[46] Subscript i denotes a primary substrate as P, a contaminant as D, and an electron acceptor as O.

References

Aamand, J., C. Jorgensen, E. Arvin, and B. K. Jensen, Microbial adaptation of degradation of hydrocarbons in polluted and unpolluted groundwater, *J. Contam. Hydrol.*, *4*, 299–312, 1989.

Albrechtsen, H., Distribution of bacteria, estimated by a viable count method, and heterotrophic activity in different size fractions of aquifer sediment, *Geomicrobiol. J.*, *12*, 253–264, 1994.

Alexander, M., *Introduction to Soil Microbiology*, 2nd ed., John Wiley, New York, 1977.

Alvarez-Cohen, L., P. L. McCarty, and P. V. Roberts, Sorption of trichloroethylene onto a zerolite accompanied by methanotrophic biotransformation, *Environ. Sci. Technol.*, *27*, 2141–2148, 1993.

Anderson, J. E., and P. L. McCarty, Model for treatment of trichloromethylene by methanotrophic biofilms, *J. Environ. Eng.*, *120*(2), 379–400, 1994.

Atlas, R. M., Microbial degradation of petroleum hydrocarbons: An environmental perspective, *Microbiol. Rev.*, *45*(1), 180–209, 1981.

Baveye, P., and A. Valocchi, An evaluation of mathematical models of the transport of biologically reacting solutes in saturated soils and aquifers, *Water Resour. Res.*, *25*(6), 1413–1421, 1989.

Bengtsson, G., R. Lindqvist, and M. D. Piwoni, Sorption of trace organics to colloidal clays, polymers, and bacteria, *Soil Sci. Soc. Am. J.*, *57*, 1261–1270, 1993.

Borden, R. C., and P. B. Bedient, Transport of dissolved hydrocarbons influenced by oxygen-limited biodegradation, 1, Theoretical development, *Water Resour. Res.*, *22*(13), 1973–1982, 1986.

Campbell, R., *Microbial Ecology*, 2nd ed., Blackwell Sci., Malden, Mass., 1983.

Chang, W. K., and C. S. Criddle, Experimental evaluation of a model for cometabolism: Prediction of simultaneous degradation of trichloroethylene and methane by a methanotrophic mixed culture, *Biotechnol. Bioeng.*, *56*(5), 492–501, 1997.

Chen, Y., L. M. Abriola, P. J. J. Alvarez, P. J. Anid, and T. M. Vogel, Modeling transport and biodegradation of benzene and toluene in sandy aquifer material, comparisons with experimental measurements, *Water Resour. Res.*, *28*(7), 1833–1847, 1992.

Chilakapati, A., T. Ginn, and J. Szecsody, An analysis of complex reaction networks in groundwater modeling, *Water Resour. Res.*, *34*(7), 1767–1780, 1998.

Clement, T. P., B. S. Hooker, and R. S. Skeen, Macroscopic models for predicting changes in saturated porous media properties caused by microbial growth, *Ground Water*, *34*(5), 934–942, 1996.

Corapcioglu, M. Y., and A. L. Baehr, A compositional multiphase model for groundwater contamination by petroleum products, 1, Theoretical consideration, *Water Resour. Res.*, *23*(1), 191–200, 1987.

Corapcioglu, M. Y., and A. Haridas, Microbial transport in soils and groundwater, a numerical model, *Adv. Water Resour.*, *8*, 188–200, 1985.

Corapcioglu, M. Y., and S. Jiang, Colloid-facilitated groundwater contaminant transport, *Water Resour. Res.*, *29*(7), 2215–2226, 1993.

Crocker, F. H., W. F. Guerin, and A. S. Boyd, Bioavailability of naphthalene sorbed to cationic surfactant-modified smectite clay, *Environ. Sci. Technol.*, *29*, 2953–2958, 1995.

Duba, A. G., K. J. Jackson, M. C. Jovanovich, R. B. Knapp, and R. T. Taylor, TCE remediation using in situ resting-state bioremediation, *Environ. Sci. Technol.*, *30*(6), 1982–1989, 1996.

Flathman, P. E., D. E. Jerger, and J. H. Exner, *Bioremediation: Field Experience*, A. F. Lewis, Boca Raton, Fla., 1994.

Gallo, C., and G. Manzini, 2-D numerical modeling of bioremediation in heterogeneous saturated soils, *Transp. Porous Media*, *31*, 67–88, 1998.

Godsy, E. M., D. F. Goerlitz, and D. Grbic-Galic, Methanogenic biodegradation of cresote contaminants in natural and simulated ground-water ecosystems, *Ground Water*, *30*(2), 232–242, 1992.

Harvey, R. W., and L. B. Barber, Associations of free-living bacteria and dissolved organic compounds in a plume of contaminated groundwater, *J. Contam. Hydrol.*, *9*, 91–103, 1992.

Harvey, R. W., R. L. Smith, and L. George, Effect of organic contamination upon microbial distributions and heterotrophic uptake in a Cape Cod, Mass. aquifer, *Appl. Environ. Microbiol.*, *48*, 1197–1202, 1984.

Hornberger, G. M., A. L. Mills, and J. S. Herman, Bacterial transport in porous media: Evaluation of a model using laboratory observations, *Water Resour. Res.*, *28*(3), 915–938, 1992.

Huesemann, M. H., and M. J. Truex, The role of oxygen diffusion in passive bioremediation of petroleum contaminated soils, *J. Hazard. Mater.*, *51*, 93–113, 1996.

Ives, K. J., and V. Pienvichitr, Kinetics of the filtration of dilute suspensions, *Chem. Eng. Sci.*, *20*, 965–973, 1965.

Jenkins, M. B., and L. W. Lion, Mobile bacteria and transport of polynuclear aromatic hydrocarbons in porous media, *Appl. Environ. Microbiol.*, *59*, 3306–3313, 1993.

Kim, S. H., and M. Y. Corapcioglu, A kinetic approach to modeling mobile bacteria-facilitated groundwater contaminant transport, *Water Resour. Res.*, *32*(2), 321–331, 1996.

Kindred, J. S., and M. A. Celia, Contaminant transport and biodegradation, 1, Conceptual model and test simulation, *Water Resour. Res.*, *25*(6), 1149–1159, 1989.

Lee, M. D., J. M. Thomas, R. C. Borden, P. B. Bedient, C. H. Ward, and J. T. Wilson, Biorestoration of aquifers contaminated with organic compounds, *Crit. Rev. Environ. Control*, *18*(1), 29–89, 1988.

Magee, B. R., L. W. Loin, and A. T. Lemley, Transport of dissolved organic macromolecules and their effect on the transport of Phenanthrene in porous media, *Environ. Sci. Technol.*, *25*, 323–331, 1991.

Mayotte, T. J., M. J. Dybas, and C. S. Criddle, Bench-scale evaluation of bioremediation to remediate carbon tetrachloride-contaminated aquifer materials, *Ground Water*, *34*(2), 358–367, 1996.

McDowell-Boyer, L. M., J. R. Hunt, and N. Sitar, Particle transport through porous media, *Water Resour. Res.*, *22*, 1901–1922, 1986.

McNab, W. W., and T. N. Narasimhan, Modeling reactive transport of organic compounds in groundwater using a partial redox disequilibrium approach, *Water Resour. Res.*, *30*(9), 1635–2619, 1994.

Molz, F. J., M. A. Widdowson, and L. D. Benefield, Simulation of microbial growth dynamics coupled to nutrient and oxygen transport in porous media, *Water Resour. Res.*, *22*(8), 1207–1216, 1986.

Murphy, E. M., T. R. Ginn, A. Chilakapati, T. Resch, J. L. Phillips, T. W. Wietsma, and C. M. Spadoni, The influence of physical heterogeneity on microbial degradation and distribution in porous media, *Water Resour. Res.*, *33*(5), 1087–1103, 1997.

Norris, R., *Handbook of Bioremediation*, A. F. Lewis, Boca Raton, Fla., 1994.

Ogram, A. V., R. E. Jessup, L. T. Ou, and P. S. C. Rao, Effects of sorption on biological degradation rates of (2,4-dichlorophenoxy) acetic acid in soils, *Appl. Environ. Microbiol.*, *49*, 582–587, 1985.

Oldenhuis, R., R. L. J. M. Vink, D. B. Janssen, and B. Witholts, Degradation of chlorinated aliphatic hydrocarbons by Methylosinus trichosporium OB3b expressing soluble methane monooxygenase, *Appl. Environ. Microbiol.*, *55*, 2819–2826, 1989.

Peyton, B. M., Improved biomass distribution using pulsed injections of electron donor and acceptor, *Water Res.*, *30*(3), 756–758, 1996.

Reddy, H. L., and R. M. Ford, Analysis of biodegradation and bacterial transport: Comparison of models with kinetic and equilibrium bacterial adsorption, *J. Contam. Hydrol.*, *22*(3–4), 271–287, 1996.

Rifai, H. S., and P. B. Bedient, Comparison of biodegradation kinetics with an instantaneous reaction model for ground water, *Water Resour. Res.*, *26*(4), 637–645, 1990.

Rittman, B. E., and P. L. McCarty, Model of steady-state-biofilm kinetics, *Biotechnol. Bioeng.*, *22*, 2343–2357, 1980.

Semprini, L., and P. L. McCarty, Comparison between model simulations and field results for in-situ biorestoration of chlorinated aliphatics, part 1, Biostimulation of methanotrophic bacteria, *Ground Water*, *29*(3), 365–374, 1991.

Semprini, L., and P. L. McCarty, Comparison between model simulations and field results for in-situ biorestoration of chlorinated aliphatics, part 2, Cometabolic transformations, *Ground Water*, *30*(1), 37–44, 1992.

Semprini, L., G. D. Hopkins, and P. V. Roberts, A field evaluation of in-situ biodegradation of chlorinated ethenes: Studies of competitive inhibition, *Ground Water*, *29*(2), 239–250, 1991.

Taylor, S. W., and P. R. Jaffé, Substrate and biomass transport in a porous medium, *Water Resour. Res.*, *26*(9), 2181–2194, 1990.

Taylor, S. W., P. C. D. Milly, and P. R. Jaffé, Biofilm growth and the related changes in the physical properties of a porous medium, 2, Permeability, *Water Resour. Res.*, *26*(9), 2161–2169, 1990.

van Loosdrecht, M. C. M., J. Lyklema, W. Norde, and A. J. B. Zehnder, Influence of interfaces on microbial activity, *Microbiol. Rev.*, *54*, 75–87, 1990.

Vandevivere, P., and P. Baveye, Saturated hydraulic conductivity reduction caused by aerobic bacteria in sand columns, *Soil Sci. Soc. Am. J.*, *56*(1), 1–13, 1992.

Vandevivere, P., P. Baveye, D. S. de Lozada, and P. DeLeo, Microbial clogging of saturated soils and aquifer materials: Evaluation of mathematical models, *Water Resour. Res.*, *31*(9), 2173–2180, 1995.

Widdowson, M. A., F. J. Molz, and L. D. Benefield, A numerical transport model for oxygen- and nitrate-based respiration linked to substrate and nutrient availability in porous media, *Water Resour. Res.*, *24*(9), 1553–1565, 1988.

Wilson, J. T., and B. H. Wilson, Biotransformation of trichloroethylene in soil, *Appl. Environ. Microbiol.*, *49*, 242–243, 1985.

ZoBell, C. E., Action of microorganisms on hydrocarbons, *Bacteriol. Rev.*, *10*, 1–49, 1946.

Zysset, A., F. Stauffer, and T. Dracos, Modeling of reactive groundwater transport governed by biodegradation, *Water Resour. Res.*, *30*(8), 2423–2434, 1994.

M. Y. Corapcioglu, Department of Civil Engineering, Texas A&M University, College Station, TX 77843-3136, USA.

S. Wang, Environmental Research Institute, Ewha Womans University, Seoul, Korea, 120-750. (sookyun@ewha.ac.kr)